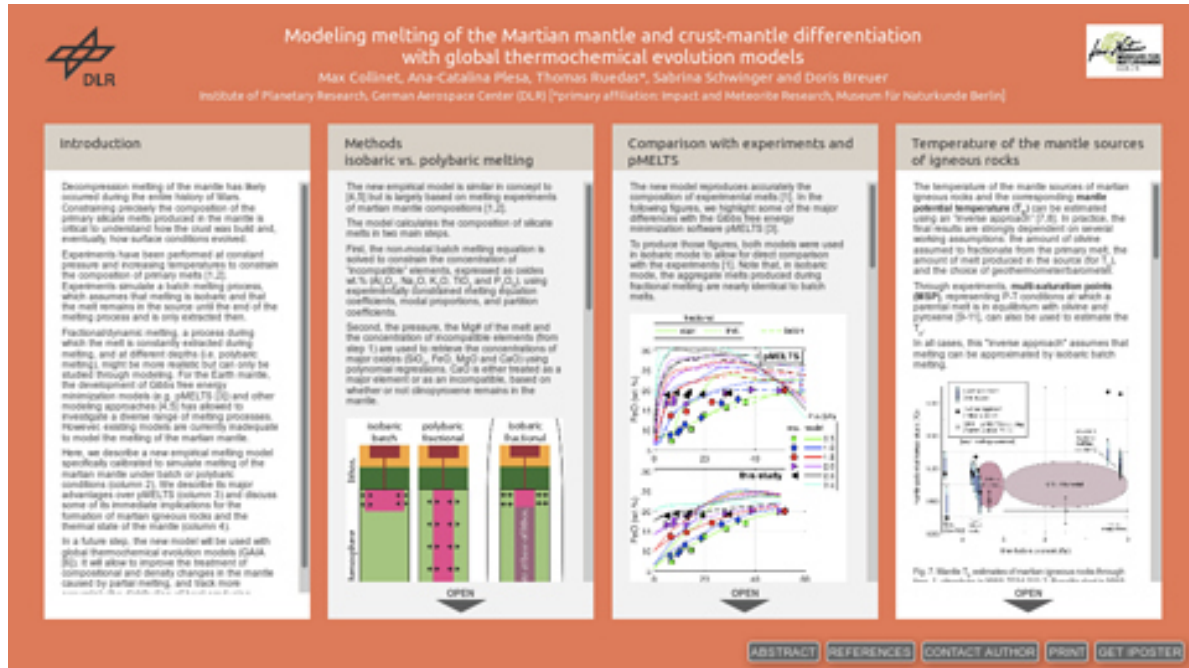


# Modeling melting of the Martian mantle and crust-mantle differentiation with global thermochemical evolution models

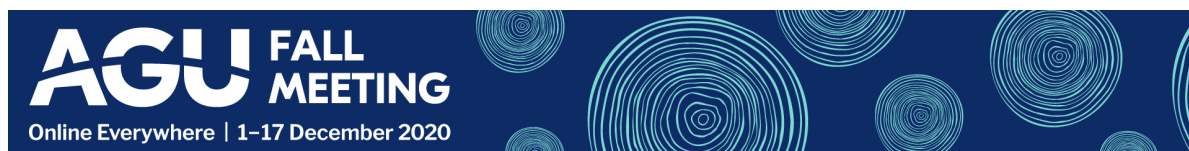


Max Collinet, Ana-Catalina Plesa, Thomas Ruedas\*, Sabrina Schwinger and Doris Breuer

Institute of Planetary Research, German Aerospace Center (DLR) [\*primary affiliation: Impact and Meteorite Research, Museum für Naturkunde Berlin]



PRESENTED AT:



## INTRODUCTION

Decompression melting of the mantle has likely occurred during the entire history of Mars. Constraining precisely the composition of the primary silicate melts produced in the mantle is critical to understand how the crust was build and, eventually, how surface conditions evolved.

Experiments have been performed at constant pressure and increasing temperatures to constrain the composition of primary melts [1,2]. Experiments simulate a batch melting process, which assumes that melting is isobaric and that the melt remains in the source until the end of the melting process and is only extracted then.

Fractional/dynamic melting, a process during which the melt is constantly extracted during melting, and at different depths (i.e. polybaric melting), might be more realistic but can only be studied through modeling. For the Earth mantle, the development of Gibbs free energy minimization models (e.g. pMELTS [3]) and other modeling approaches [4,5] has allowed to investigate a diverse range of melting processes. However, existing models are currently inadequate to model the melting of the martian mantle.

Here, we describe a new empirical melting model specifically calibrated to simulate melting of the martian mantle under batch or polybaric conditions (column 2). We describe its major advantages over pMELTS (column 3) and discuss some of its immediate implications for the formation of martian igneous rocks and the thermal state of the mantle (column 4).

In a future step, the new model will be used with global thermochemical evolution models (GAIA [6]). It will allow to improve the treatment of compositional and density changes in the mantle caused by partial melting, and track more accurately the distribution of heat producing elements between the mantle and the crust.

## METHODS

### ISOBARIC VS. POLYBARIC MELTING

The new empirical model is similar in concept to [4,5] but is largely based on melting experiments of martian mantle compositions [1,2].

The model calculates the composition of silicate melts in two main steps.

First, the non-modal batch melting equation is solved to constrain the concentration of “incompatible” elements, expressed as oxides wt.% ( $\text{Al}_2\text{O}_3$ ,  $\text{Na}_2\text{O}$ ,  $\text{K}_2\text{O}$ ,  $\text{TiO}_2$  and  $\text{P}_2\text{O}_5$ ), using experimentally constrained melting equation coefficients, modal proportions, and partition coefficients.

Second, the pressure, the Mg# of the melt and the concentration of incompatible elements (from step 1) are used to retrieve the concentrations of major oxides ( $\text{SiO}_2$ ,  $\text{FeO}$ ,  $\text{MgO}$  and  $\text{CaO}$ ) using polynomial regressions.  $\text{CaO}$  is either treated as a major element or as an incompatible, based on whether or not clinopyroxene remains in the mantle.

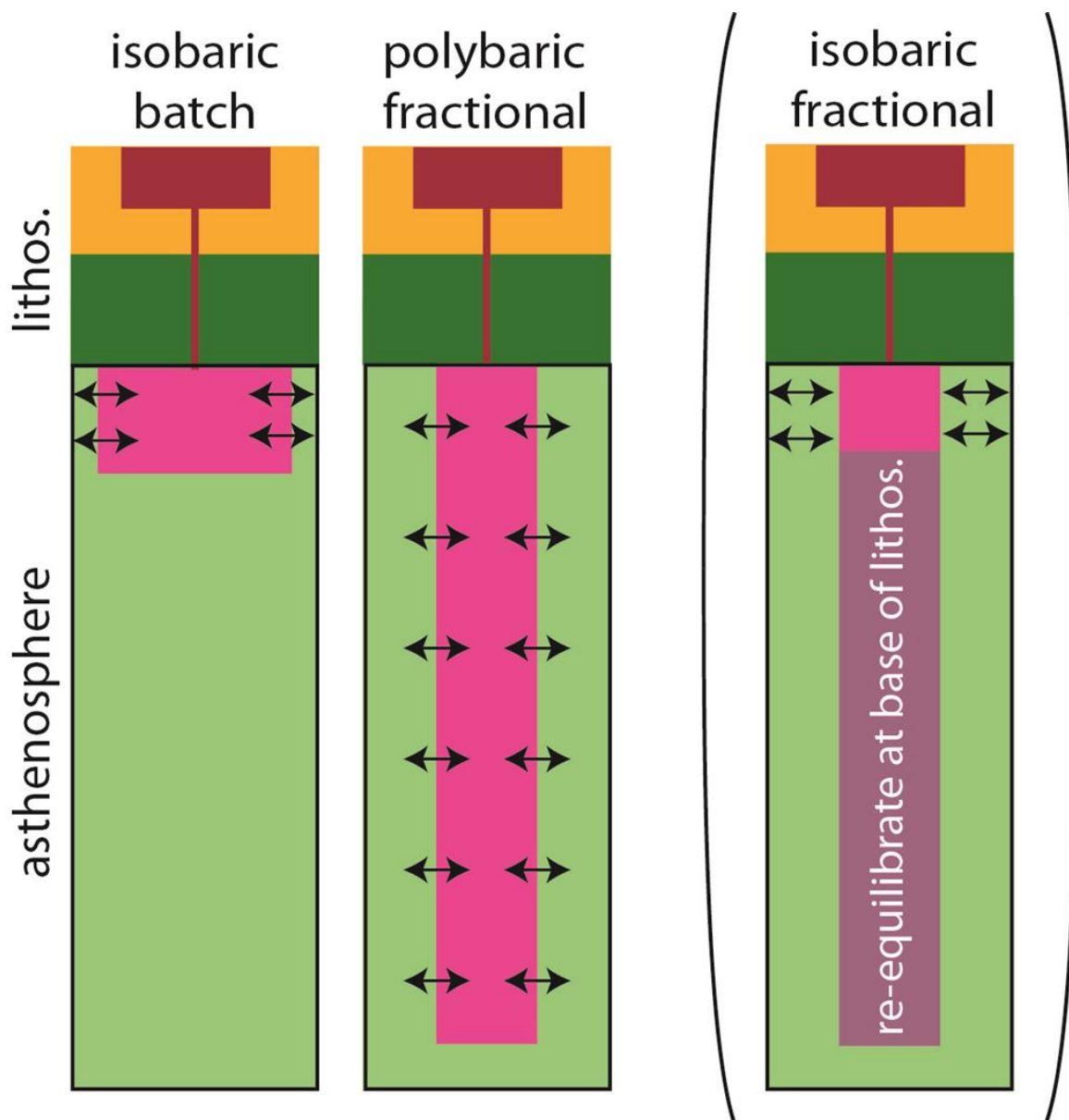


Fig. 1. The model can be used to simulate different melting processes

In **isobaric batch** melting mode, the melt fraction, the pressure and the mantle bulk composition are provided as input and the model returns the composition of the melt, the temperature at which the melt is in equilibrium with the mantle and the corresponding **mantle potential temperature ( $T_p$ )**. The melting process is assumed to occur at constant pressure in a single “batch”, and no melt is removed until melting is over.

In **polybaric fractional** melting mode, the mantle potential temperature, the mantle bulk composition, and the pressure at which melting ends (i.e. the base of the lithosphere) are provided as inputs. The model calculates the solidus temperature as a function of pressure and returns the pressure at which melting begins. The compositions of small melt increments (i.e. **instantaneous melts**) are calculated and extracted from the residue above an adjustable **retained “critical” melt fraction** (0.4-2 wt.%; the model is therefore “near-fractional” or “dynamic”). The model repeats those iterations while decreasing the pressure. The new solidus and the new ambient mantle temperature are constantly adjusted. Melting continues up to the imposed lower pressure, representing the base of the lithosphere. At this point, all melt increments produced at different depths are pooled as a single **aggregate melt**.

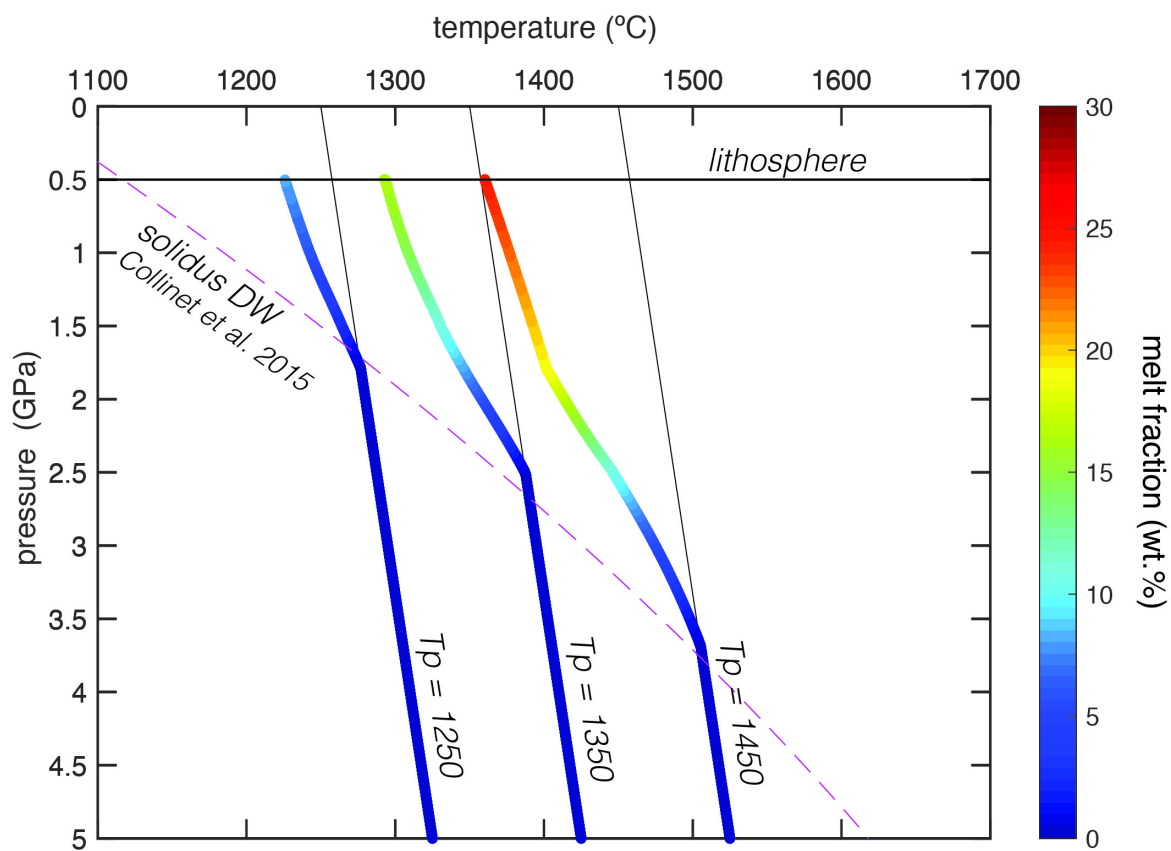


Fig. 2. Example of fractional polybaric melting (decompression melting) along three adiabats.

This latter melting mode can also be used at constant pressure to simulate **isobaric fractional melting**. This melting process can be envisioned as a melting column extending down to a certain depth and affected by fractional melting but with re-equilibration of all melt increments at the base of the lithosphere.

## COMPARISON WITH EXPERIMENTS AND PMELTS

The new model reproduces accurately the composition of experimental melts [1]. In the following figures, we highlight some of the major differences with the Gibbs free energy minimization software pMELTS [3].

To produce those figures, both models were used in isobaric mode to allow for direct comparison with the experiments [1]. Note that, in isobaric mode, the aggregate melts produced during fractional melting are nearly identical to batch melts.

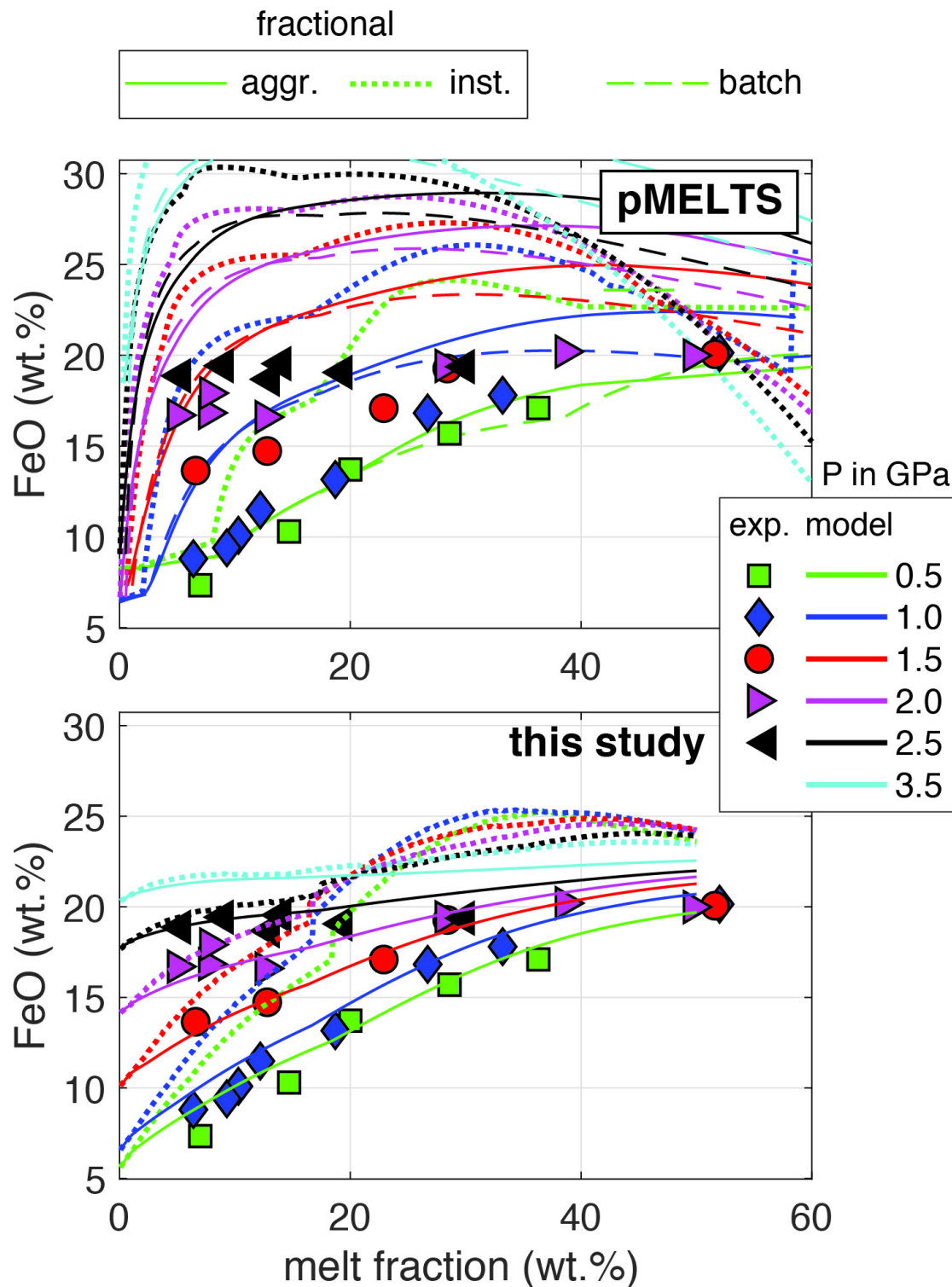


Fig. 3. Compared to the experiments [1] and the new model, pMELTS overestimates the **FeO content of silicate melts** by ~4 wt.% (1.0 GPa) to ~8

wt.% (2.5 GPa), and possibly as much as ~10 wt.% (3.5 GPa). As a result, the density of silicate melts is overestimated by up to 200 kg/m<sup>3</sup> and the density of the mantle residue is underestimated by up to 40 kg/m<sup>3</sup>.

pMELTS systematically underestimates the SiO<sub>2</sub> melt concentrations and overestimates the FeO and MgO concentrations.

Using pMELTS data together with geodynamical models thus leads to significant errors in the density contrasts of the melting products (melts and residues) relative to the ambient mantle. Those errors can impact mantle convection and melt segregation (Fig. 3).

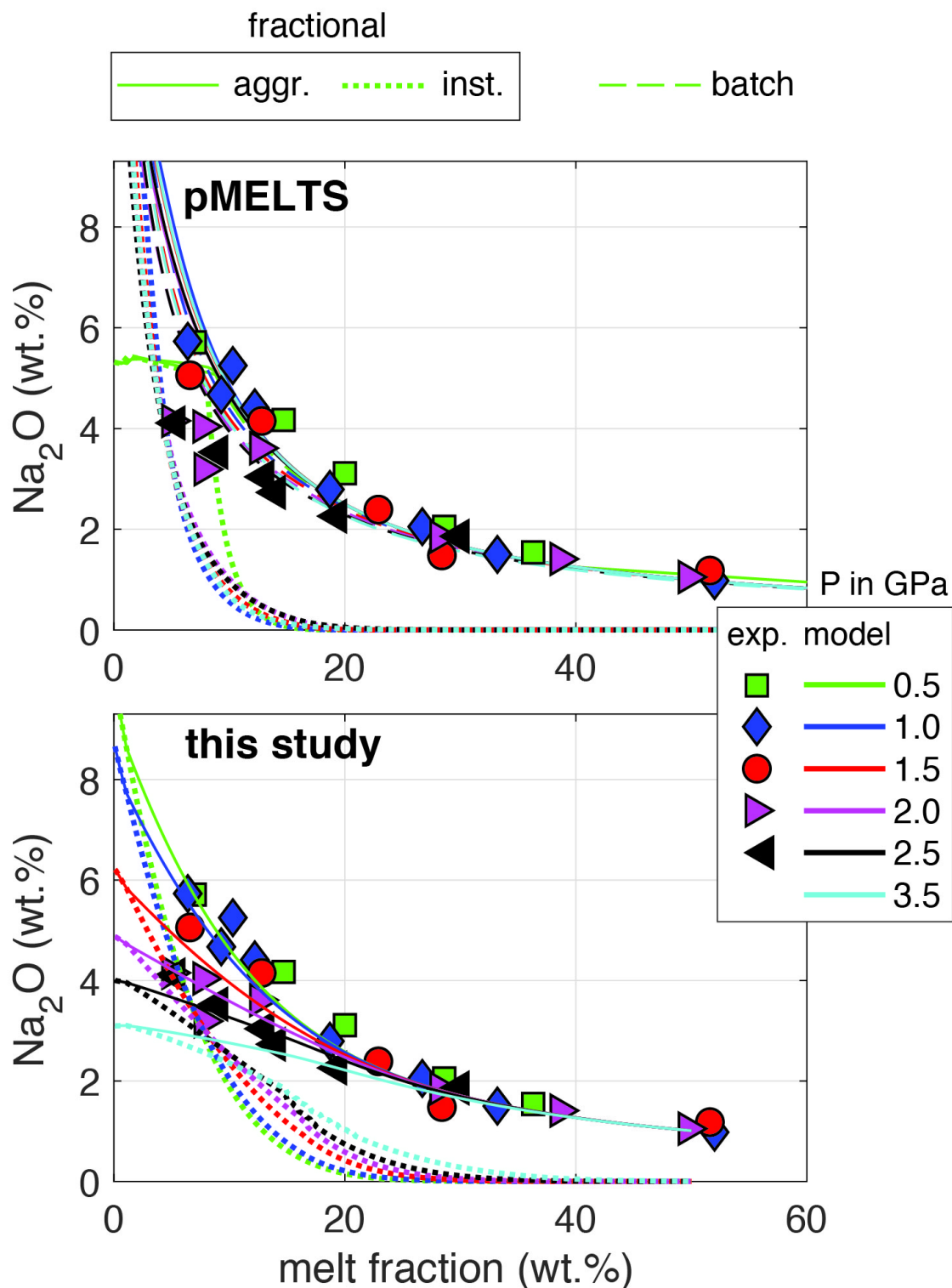


Fig. 4. pMELTS does not accurately account for the increase of Na<sub>2</sub>O compatibility in pyroxene with increasing pressure. The Na<sub>2</sub>O concentration of the resulting melts are overestimated at high pressure.

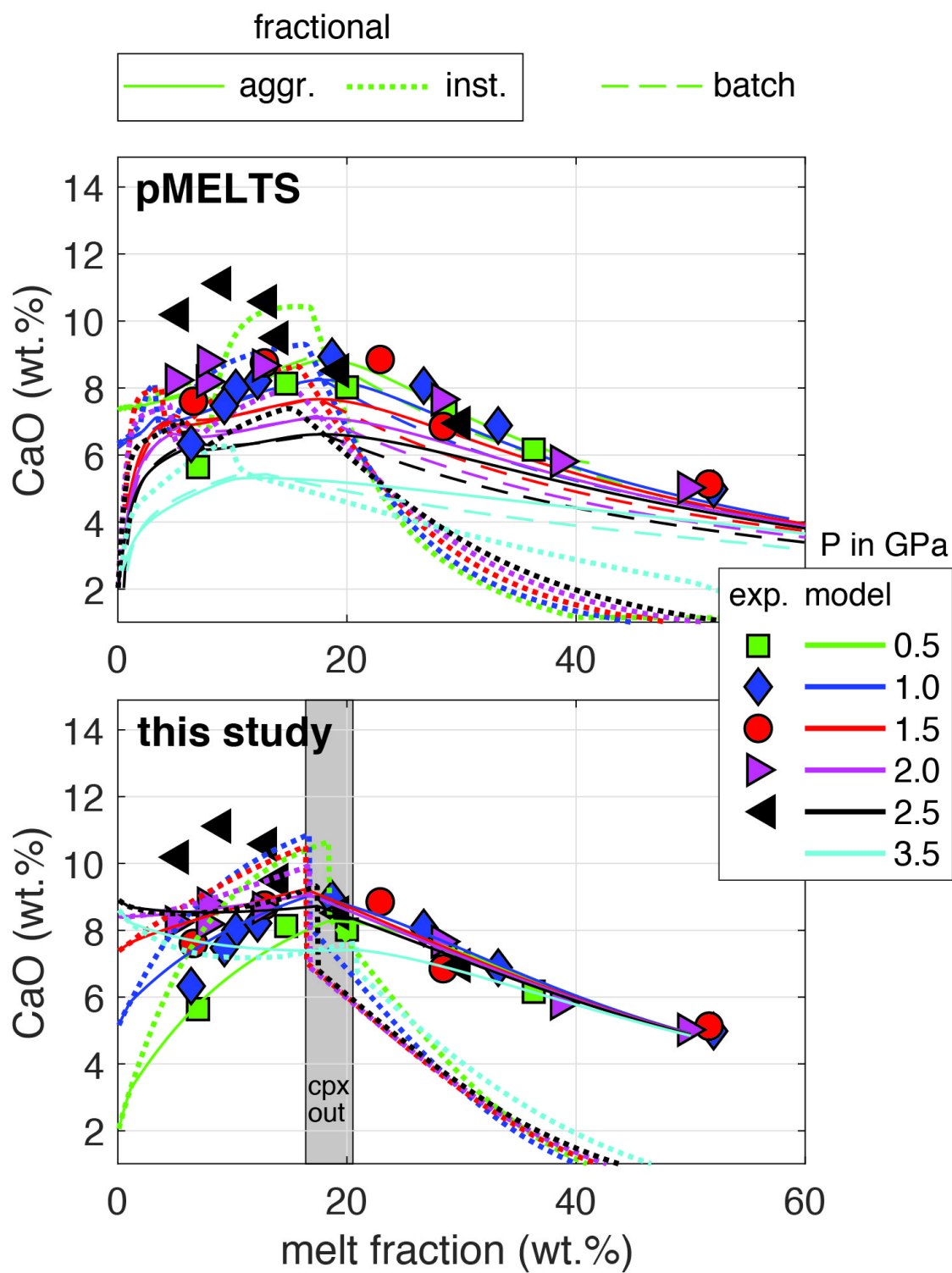


Fig. 5. CaO is treated either as a major oxide or an incompatible in the empirical model. The transition occurs when clinopyroxene is completely consumed (i.e. lherzolite to harzburgite transition). In both models, the **CaO concentration of melts** increases until clinopyroxene disappears (cpx-out), and then decreases rapidly in the instantaneous melts. The CaO concentration is highest at the spinel- to garnet- lherzolite transition (~2.5 GPa) in experiments and the empirical model while pMELTS erroneously predicts a continuous decrease of the CaO content with increasing pressure, for a given melt fraction.



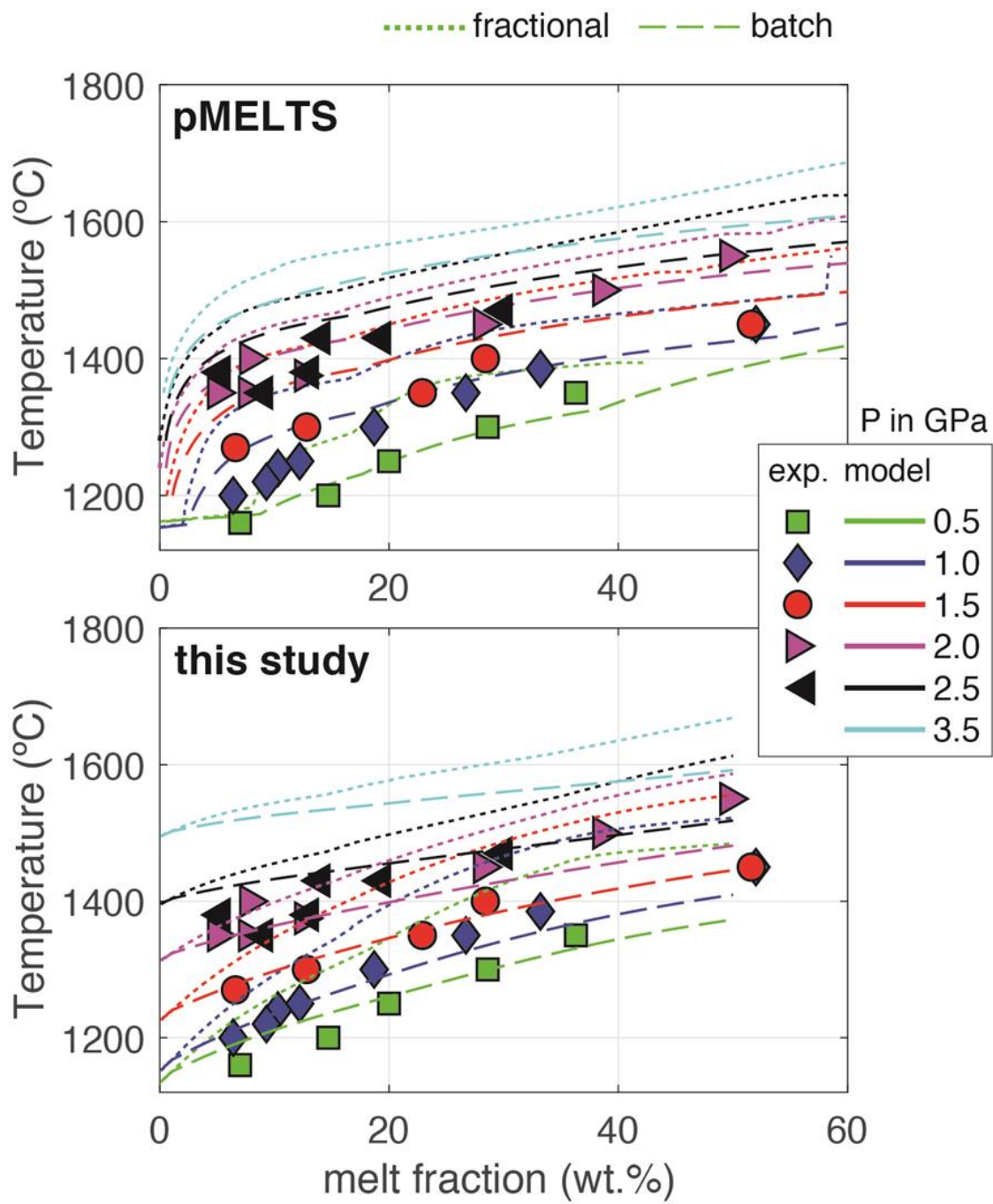


Fig. 6. Solidus temperature and increase of the melt fraction with temperature.



# TEMPERATURE OF THE MANTLE SOURCES OF IGNEOUS ROCKS

The temperature of the mantle sources of martian igneous rocks and the corresponding **mantle potential temperature ( $T_p$ )** can be estimated using an “inverse approach” [7,8]. In practice, the final results are strongly dependent on several working assumptions: the amount of olivine assumed to fractionate from the primary melt, the amount of melt produced in the source (for  $T_p$ ), and the choice of geothermometer/barometer.

Through experiments, **multi-saturation points (MSP)**, representing P-T conditions at which a parental melt is in equilibrium with olivine and pyroxene [9-11], can also be used to estimate the  $T_p$ .

In all cases, this “inverse approach” assumes that melting can be approximated by isobaric batch melting.

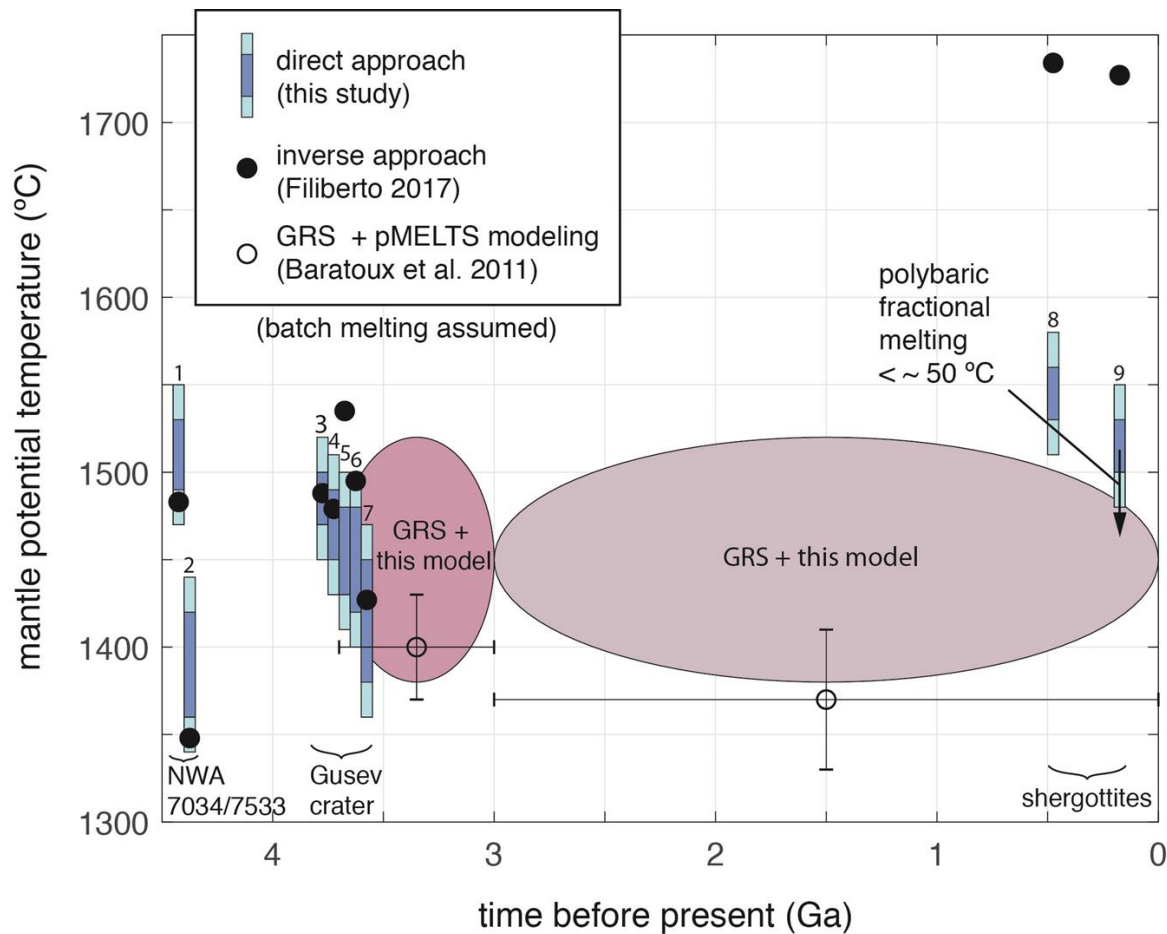


Fig. 7. Mantle  $T_p$  estimates of martian igneous rocks through time. 1, vitrophyre in NWA 7034 [11]; 2, Basaltic clast in NWA 7533 [12]; 3, Fastball; 4, Irvine; 5, Adirondack class basalts; 6, Ace; 7, Humble peak; 8, depleted shergottites; 9, enriched shergottites. The center blue bars represent the range of  $T_p$  of successful simulations. The outer cyan bars represent an additional  $\pm 20$  °C model uncertainty (not yet fully characterized). Several compositions can also be matched by polybaric fractional melting. When this is the case, the  $T_p$  is  $\sim 50$  °C lower than the corresponding batch melting simulation (also see below). The pink ellipses represent the new  $T_p$  estimates for GRS volcanic provinces [13], when the new model is used instead of pMELTS. They account for both batch and polybaric melting (Fig. 8 and 9).

The new model can be used to re-evaluate the temperature of the mantle sources of igneous rocks using a “direct approach”. Some model parameters were varied systematically ( $T_p$ , P) while others were varied through initial guesses followed by a random search around an average value (bulk mantle composition). The results are compared to igneous rocks which are in equilibrium with, or contain, olivine Fo<sub>75-85</sub> (after the addition of 0-10 wt.% olivine; Fig. 7) and are therefore assumed to be in equilibrium with the martian mantle.

An important difference between the new model and some previous  $T_p$  estimates [8] is that we find that shergottites parental

melts can be produced at relatively shallow conditions (1.0-1.5 GPa), and therefore much cooler  $T_p$ , consistent with MSP experiments [9,11].

Previous  $T_p$  estimates for GRS volcanic provinces are likely underestimated due to errors in the FeO and SiO<sub>2</sub> concentrations of the melts introduced by pMELTS and which could not be completely accounted for [13].

Although GRS data provide the concentrations of a limited number of elements (e.g. Fe, Si, Th), the new model can be used to update semi-quantitatively the  $T_p$  estimates (Fig. 8 and 9).

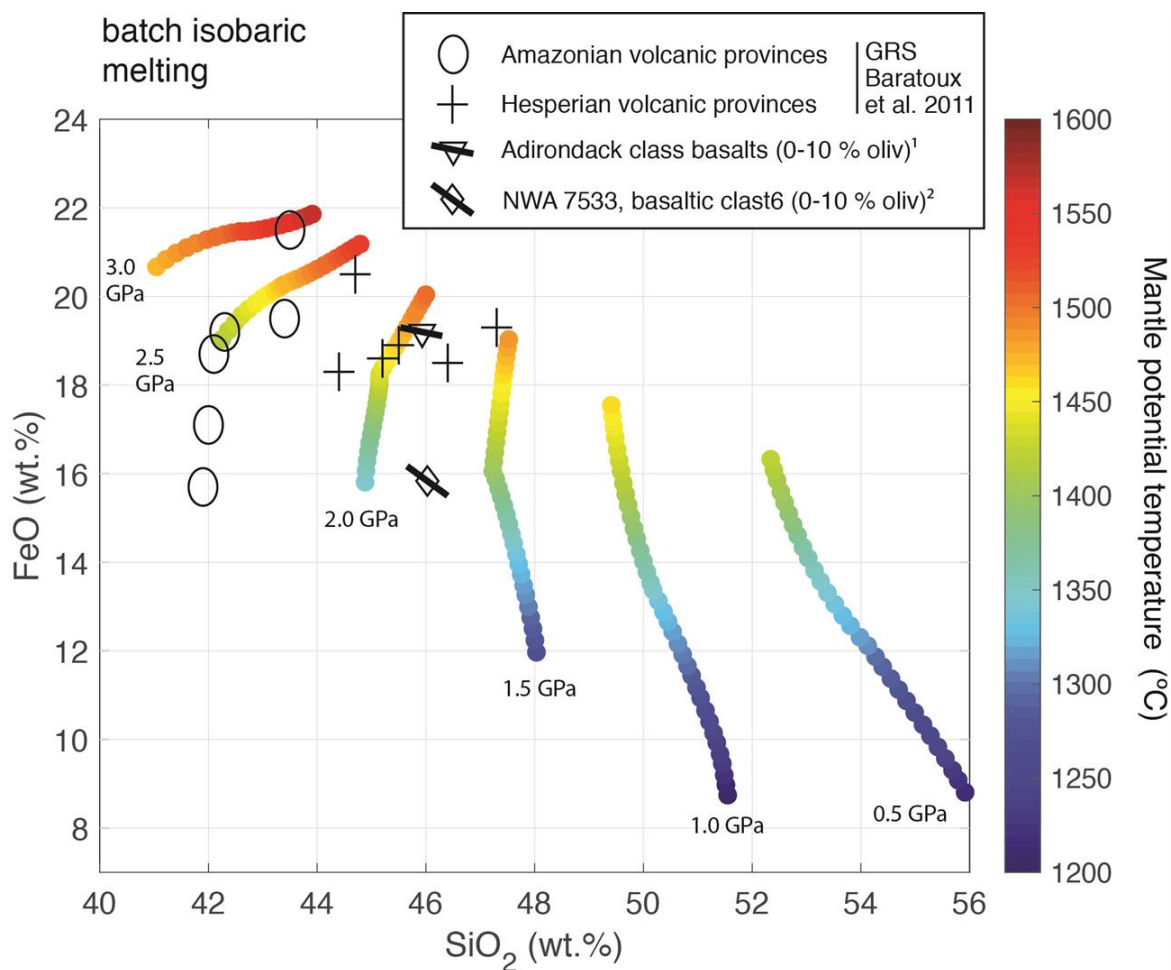


Fig. 8. Possible range of melting conditions for GRS volcanic provinces from [13], assuming isobaric batch melting and a DW mantle composition [14]. Each trajectory represents a specific pressure of melting and increasing  $T_p$  (total melt fraction between 3 and 30 wt.%). The black lines on NWA 7533 and Adirondack basalt symbols represent the effect of adding back 0 to 10 wt.% olivine.

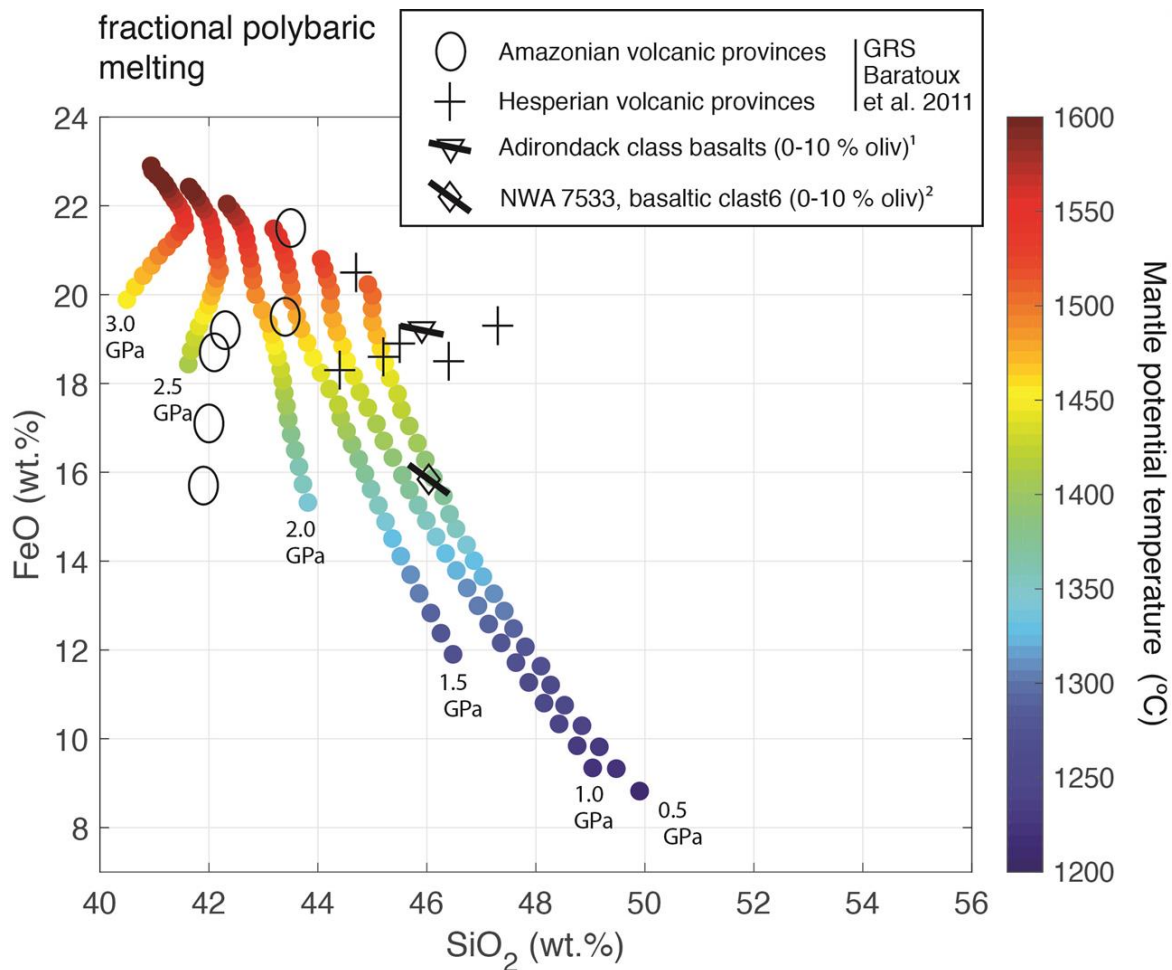


Fig. 9. Possible range of melting conditions for GRS volcanic provinces from [13], assuming polybaric fractional melting and a DW mantle composition [14]. Each trajectory represents a specific pressure at the base of the lithosphere, the pressure at which polybaric melting ends. The pressure at which melting starts (not represented) increases with the  $T_p$  (total melt fraction between 3 and 30 wt.%).

### Polybaric melting

The composition of certain igneous rocks can also be matched by polybaric fractional melting:

- Adirondack class basalts + 7 wt.% olivine

DW mantle,  $T_p = 1430$  °C,  $P = 3.3$  to  $0.7$  GPa

- NWA 7533 basaltic clast + 10 wt.% olivine

DW mantle,  $T_p = 1400$  °C,  $P = 2.7$  to  $0.7$  GPa

- LAR 06319 / NWA 1068 + 5 wt.% olivine

depleted mantle,  $T_p = 1470$  °C,  $P = 2.6$  to  $0.7$  GPa

In those cases, the mantle  $T_p$  are 40-60 °C lower compared to isobaric batch cases and ~100 °C lower compared to isobaric fractional cases.

### Implications

Collectively, the new  $T_p$  estimates indicate that the temperature of the mantle sources of sampled igneous rocks was relatively stable over time. In recent times, partial melting was probably limited to the hottest mantle plumes localized under major martian volcanoes in the Tharsis and Elysium regions, while much of the mantle could be too cold to melt. In earlier stages of Mars' history, a thinner crust and lithosphere could have allowed plumes of contrasting temperatures to produce melts. However, not all early primary melts were recorded at the surface. The hottest plumes could have produced melts of neutral or negative buoyancy. In addition, subsequent volcanism and other geological processes likely concealed some of the early surface expressions of primary mantle melts.

Therefore, a stable  $T_p$  of the mantle sources of martian igneous rocks is most likely not representative of the average mantle  $T_p$  and should not be interpreted as conflicting with the secular cooling of the mantle.

## ABSTRACT

Basaltic melts are produced when convection adiabatically brings deep and hot mantle to lower pressures. Such primary melts were extracted from the mantle of Mars, crystallized near the surface and progressively built the Martian crust. This process displaced a large fraction of the heat producing elements from the mantle to the crust and created an insulating layer that slowed down further cooling of the mantle. The complex crust-mantle system controlled many aspects of the geologic history of Mars, including the development of an atmosphere and whether conditions favorable to life could have existed.

Our knowledge of the mineralogy, chemical composition and physical properties of the crust of Mars is rapidly expanding. Global geodynamical models can be used to interpret the available data and constrain the processes of crust-mantle differentiation. However, existing models still treat melting in a simplified way. For example, the degree of melting is often assumed to increase linearly above the solidus temperature, while the density of the residue is assumed to decrease linearly. Calculating the density of the residual mantle more accurately is critical because the compositional buoyancy that develops during partial melting fundamentally modifies mantle dynamics.

Here, we present an improved parametrization of partial melting of the Martian mantle, which will be combined with the convection code Gaia. We created a new empirical model of melting that calculates the composition of the extracted melts and, when combined to thermodynamic models (e.g., `Perple_X`), the density of the corresponding residual mantle.

Another advantage of the new melting parametrization is that the major-element composition of partial melts can be tracked and used to constrain the petrogenesis of surface rocks. Preliminary results will be compared to available Martian rocks believed to represent primary mantle melts or melts affected by minor fractional crystallization.

## REFERENCES

- [1] Collinet, M., Médard, E., Charlier, B., Vander Auwera, J., & Grove, T. L. (2015). Melting of the primitive martian mantle at 0.5–2.2 GPa and the origin of basalts and alkaline rocks on Mars. *Earth and Planetary Science Letters*, 427(0), 83–94. <https://doi.org/http://dx.doi.org/10.1016/j.epsl.2015.06.056>
- [2] Ding, S., Dasgupta, R., & Tsuno, K. (2020). The Solidus and Melt Productivity of Nominally Anhydrous Martian Mantle Constrained by New High Pressure-Temperature Experiments - Implications for Crustal Production and Mantle Source Evolution. *Journal of Geophysical Research: Planets*, e2019JE006078. <https://doi.org/10.1029/2019JE006078>
- [3] Ghiorso, M. S., Hirschmann, M. M., Reiners, P. W., & Kress III, V. C. (2002). The pMELTS: A revision of MELTS for improved calculation of phase relations and major element partitioning related to partial melting of the mantle to 3 GPa. *Geochem. Geophys. Geosyst.*, 3(5), 1030. <https://doi.org/10.1029/2001gc000217>
- [4] Kinzler, R. J., & Grove, T. L. (1992). Primary magmas of mid-ocean ridge basalts 1. Experiments and methods. *Journal of Geophysical Research*, 97(B5), 6885–6906. <https://doi.org/10.1029/91JB02840>
- [5] Till, C. B., Grove, T. L., & Krawczynski, M. J. (2012). A melting model for variably depleted and enriched lherzolite in the plagioclase and spinel stability fields. *J. Geophys. Res.*, 117(B6), B06206. <https://doi.org/10.1029/2011jb009044>
- [6] Hüttig, C., Tosi, N., & Moore, W. B. (2013). An improved formulation of the incompressible Navier–Stokes equations with variable viscosity. *Physics of the Earth and Planetary Interiors*, 220, 11–18. <https://doi.org/https://doi.org/10.1016/j.pepi.2013.04.002>
- [7] Filiberto, J., & Dasgupta, R. (2011). Fe<sup>2+</sup>-Mg partitioning between olivine and basaltic melts: Applications to genesis of olivine-phyric shergottites and conditions of melting in the Martian interior. *Earth and Planetary Science Letters*, 304(3–4), 527–537. <https://doi.org/10.1016/j.epsl.2011.02.029>
- [8] Filiberto, J. (2017). Geochemistry of Martian basalts with constraints on magma genesis. *Chemical Geology*, 466, 1–14. <https://doi.org/https://doi.org/10.1016/j.chemgeo.2017.06.009>
- [9] Filiberto, J., Musselwhite, D. S., Gross, J., Burgess, K., Le, L., & Treiman, A. H. (2010). Experimental petrology, crystallization history, and parental magma characteristics of olivine-phyric shergottite NWA 1068: Implications for the petrogenesis of “enriched” olivine-phyric shergottites. *Meteoritics & Planetary Science*, 45(8), 1258–1270. <https://doi.org/10.1111/j.1945-5100.2010.01080.x>
- [10] Monders, A. G., Médard, E., & Grove, T. L. (2007). Phase equilibrium investigations of the Adirondack class basalts from the Gusev plains, Gusev crater, Mars. *Meteoritics & Planetary Science*, 42(1), 131–148. <https://doi.org/10.1111/j.1945-5100.2007.tb00222.x>
- [11] Udry, A., Lunning, N. G., McSween Jr, H. Y., & Bodnar, R. J. (2014). Petrogenesis of a vitrophyre in the martian meteorite breccia NWA 7034. *Geochimica et Cosmochimica Acta*, 141(0), 281–293. <https://doi.org/http://dx.doi.org/10.1016/j.gca.2014.06.026>
- [12] Santos, A. R., Agee, C. B., McCubbin, F. M., Shearer, C. K., Burger, P. V, Tartèse, R., & Anand, M. (n.d.). Petrology of igneous clasts in Northwest Africa 7034: Implications for the petrologic diversity of the martian crust. *Geochimica et Cosmochimica Acta*, 0. <https://doi.org/http://dx.doi.org/10.1016/j.gca.2015.02.023>
- [13] Baratoux, D., Toplis, M. J., Monnereau, M., & Gasnault, O. (2011). Thermal history of Mars inferred from orbital geochemistry of volcanic provinces. *Nature*, 472(7343), 338–341. <https://doi.org/10.1038/nature09903>
- [14] Dreibus, G., & Wanke, H. (1985). Mars, a volatile-rich planet. *Meteoritics*, 20(2), 367–381.